Mechanism for Carbon Transfer From Magnesia-Graphite Ladle Refractories to Ultralow-Carbon Steel

Mechanisms of carbon transport between magnesia-graphite ladle refractories and ultralow-carbon steel were investigated using laboratory dip tests with commercial ladle refractories in a vacuum induction furnace. The reacted refractories were examined by scanning electron microscopy and energy-dispersive x-ray spectroscopy analysis to observe changes in the refractory that influenced the rate of carbon pickup to the steel.




Authors

Andrew A. Russo (top row, left)
liaison/MRB engineer II, GKN Aerospace, Hazelwood, Mo., USA
aarrk5@mst.edu

Jeffrey D. Smith (top row, right)
associate professor of ceramic engineering, Missouri University of Science and Technology, Rolla, Mo., USA
jsmith@mst.edu

Ronald J. O'Malley (bottom row, left)
F. Kenneth Iverson Chair, professor and director, Kent D. Peaslee Steel Manufacturing Research Center, Missouri University of Science and Technology, Rolla, Mo., USA
omalleyr@mst.edu

Von L. Richards (bottom row, right)
Robert W. Wolf Professor of Metallurgical Engineering, Department of Materials Science and Engineering, Missouri University of Science and Technology, Rolla, Mo., USA
vonlr@mst.edu

Ultralow-carbon (ULC) steels are used in processes where maximum ductility is required such as forming and drawing operations, given that interstitial carbon adds strength, but lowers ductility.[1] ULC steels are classified as steels having less than 50 ppm carbon.[2] This strict requirement for carbon requires that carbon transfer from outside sources into the steel must be controlled to ensure that carbon remains within specification. Amavis reports on a French steel plant that had 20–30 ppm pickup when the aim carbon was less than 50 ppm.[2] Outside sources of carbon include alloying additions, electrodes, mold powders, tundish fluxes and refractories.[1–3] Ladle refractories often contain carbon in the form of graphite. Graphite is used because it gives the refractory excellent resistance to corrosion from molten slag, it has good wear resistance and strength at high temperature, it has a low density, and it has excellent resistance to thermal shock.[4–9] The negative aspects of using carbon-containing refractories are wear by decarburization, skull formation and temperature loss from high thermal conductivity, carbon monoxide corrosion of safety lining, and carbon pickup.[4] Steels with less carbon, such as ULC steels, have greater carbon pickup because there is a greater driving force for carbon transfer to the steel.[10] Also, lower-carbon steels wet graphite better than higher-carbon steels, so there is added contact area for carbon pickup to occur with lower-carbon steels.[10] ULC steels remain in contact with carbon-containing refractories from the degassing step to the completion of the casting step in the steelmaking process and, therefore, are subject to carbon pickup throughout this period of contact with the ladle.

The mechanisms by which carbon transports from refractory to steel must be understood so that they may be controlled. Carbon in contact with steel can be directly dissolved into the liquid steel:

$$C_s \rightarrow \underline{C} \qquad \text{(Eq. 1)}$$

Carbon contact with steel can be increased by penetration of steel into carbon-containing refractories and by corrosion of the refractory oxides. Another path for carbon transport into steel is the dissociation of carbon monoxide:

$$CO_g \rightarrow \underline{C} + \underline{O} \qquad \text{(Eq. 2)}$$

Carbon monoxide can form from carbothermic reduction of refractory oxides such as MgO or through reactions with oxides in slag, such as FeO and MnO:

$$MgO_s + C_s \rightarrow Mg_g + CO_g \qquad \text{(Eq. 3)}$$

$$FeO_{slag} + C_s \rightarrow Fe_l + CO_g \qquad \text{(Eq. 4)}$$

According to the literature, carbon dissolution is the most significant contribution of carbon pickup from ladle refractories.[2,5,11] Carbon dissolution into steel has two steps. First, carbon must dissociate from its base structure and enter the liquid steel at the steel-carbon

interface. Then, mass transfer must occur to transport the carbon from the interface into the bulk liquid steel. Many investigators have observed that mass transfer is the rate limiting step for carbon dissolution into molten steel.[7,12–17] Jansson et al. found carbon pickup from MgO-C refractory during a three-hour rotary dip test in ULC Al-killed steel was greatly dependent on convection; C pickup was 0.008 wt.% at 0 rpm rotational speed and 0.179 wt.% at 800 rpm.[17] Khanna et al. found that the dissociation of carbon from its structure may be rate controlling at first, but the reaction speeds up quickly to make mass transfer rate controlling.[12]

Steel penetration can increase contact between steel and graphite in refractories. Khanna et al. found that a drop of iron placed on an Al_2O_3-10 wt.% C specimen in an argon atmosphere for three hours penetrated 1.5 mm and picked up 5,000 ppm carbon.[6] Refractory oxides are normally non-wetting to steel. Thus, an increase in oxide content can limit steel-graphite contact by limiting penetration.[15,18] A decarburized layer at the refractory surface can also prevent steel from contacting carbon in MgO-C refractories when the remaining pore size is small and the steel is non-wetting to MgO. Bannenberg found that carbon pickup was 275 ppm on the first dip of a 3.8 wt.% C dolomite refractory rod into steel and only 25 ppm on the second dip due to decarburized layer formation.[20]

Magnesium vapor reacting with oxygen at the refractory steel interface can prevent carbon pickup by creating a dense MgO barrier layer between steel and carbon. Unkilled steel in contact with MgO-C refractory shows continuous growth of a dense MgO layer in the refractory because oxygen is readily available to oxidize the Mg vapor generated by the carbothermic reduction of MgO within the refractory.[5] As a result, unkilled steel picks up carbon quickly at first and then the carbon pickup stops once a dense MgO layer develops.[5] Al-killed steel in contact with MgO-C refractory shows rapid growth of a dense MgO layer initially, but the layer ceases to grow later due to a lack of available oxygen.[5] As a result, carbon pickup in Al-killed steel is rapid at first and then slows. Carbon pickup does not stop completely because the dense MgO layer is not continuously regenerated and cracks in the dense layer allow some contact between graphite and steel.[5]

Potschke proposed that CO gas evolution from the reaction of MgO and carbon within the refractory blocks contact between graphite and steel in unkilled steels by preventing steel penetration. However, Lehmann et al. only observed a dense layer and no CO bubbling in their experiments.[5] In contrast, Mukai et al. observed that bubble formation increased refractory corrosion and that Al additions limited gas bubble formation.[21] Aksel'rod et al. observed that carbon in the refractory prevented metal penetration by providing a physical barrier and by creating CO bubbles and gaseous oxide reaction products, which limited the wetting of steel to graphite.[22]

Slag infiltration can prevent steel from contacting carbon to inhibit carbon pickup.[19,20] However, slag can also corrode MgO grains in the refractory and lead to exposure of graphite, which can then dissolve into steel.[21,23] Thus, some carbon pickup can be directly correlated to refractory wear.[2,23] Slag wets the refractory to dissolve the oxide, and steel then wets and dissolves the exposed graphite.[10,21,24] Dissolution of MgO into the slag has been identified as the rate-controlling step for refractory erosion in the presence of slag. Therefore, increasing the resistance of MgO to slag attack and reducing the contact between the slag and MgO can limit corrosion.[10,11,21,25] Akkurt found that decreasing wetting between the refractory and slag reduced slag corrosion.[9] Refractories that employ larger MgO grains have also been found to exhibit better slag resistance because they have less surface area to attack.[19,26] MgO-saturated slags also inhibit dissolution of MgO grains.[9,19,23,27] Basic slags with lower MgO solubility can also limit MgO corrosion.[9,23,28,29] Slag MgO solubility increases with decreasing basicity, increasing alumina, increasing temperature and increasing FeO.[30] Sintered MgO has been observed to have less slag erosion resistance than fused MgO due to the presence of intergranular silicates, which assist slag penetration.[29,33] Porosity, higher temperatures and longer contact times also increase slag penetration.[31,32,33] Akkurt et al. and Resende et al. found that increasing carbon content reduces slag attack because carbon limits slag contact with oxide and prevents slag penetration.[9,25,28]

Corrosion of MgO-C refractories is enhanced when slags are strongly stirred.[13,23,34] Stirring enhances the convective mass transport of MgO in the slag. Stirring can also cause erosion of MgO grains and increased penetration of slag in refractories.[26,34] As a result, induction furnace tests can exhibit refractory corrosion rates 3 to 5 times greater than tests performed in resistance furnaces.[26,35]

While carbon loss by oxidation can inhibit steel penetration, it can also make refractories more susceptible to corrosion through slag infiltration.[1] Oxidation resistance can be increased with less carbon, larger graphite flake size and lower porosity.[36] A lower partial pressure of oxygen can protect carbon from oxidation. Akkurt et al. observed that adding 5% CO to their Ar atmosphere reduced MgO-C wear by lowering the partial pressure of oxygen.[9]

Carbon transport by CO can occur when CO is created by reduction of refractory or slag oxides by carbon.[19] These reactions are shown in Equations 3 and 4. The reduction of MgO by carbon in MgO-C

refractories is a significant source of CO.[5] Steel pressure can suppress this reaction on the ladle walls and bottom.[19]

Other methods for controlling carbon pickup have also been reported. Franken et al. found that the spread of carbon pickup from carbon-containing refractories was too great and unpredictable for use in ULC steels, which forced a change to carbon-free refractories.[4] Tassot et al. switched from 3 wt.% C dolomite bricks in the ladle body to 1 wt.% C, but the carbon pickup only dropped from 4 ppm to 2 ppm, which prompted them to change to carbonless bricks in the body.[39] Fired dolomite, $MgO\text{-}Al_2O_3$, fired spinel, magnesia-chromite and bauxite refractories have been used to replace carbon-containing refractories with some success.[2–4,29,39] Other changes can be made that allow the continued use of carbon-containing refractories. Low-carbon bricks can be decarburized at the hot face and sintered to form a barrier.[2] Using more corrosion-resistant refractory components like ZrO_2 and BN can lower the corrosion rate, thereby lowering carbon pickup.[21,40]

Given the wide industry use of MgO-C refractories in the production of ULC steels, the goal of this investigation is to determine the controlling mechanisms for carbon pickup from ladle refractories by performing experiments that attempt to reproduce the conditions present while ULC steel and ladle slag are in contact with the ladle refractory. This was accomplished by conducting refractory dip tests in a vacuum induction furnace (VIF) under an Ar atmosphere using different refractory and slag compositions and ULC steel. The refractories examined were MgO-C with 4 wt.% C, 6 wt.% C, 10 wt.% C and 12 wt.% C. The three heat conditions tested were ULC steel with no slag, ULC steel with slag and ULC steel with an MgO-saturated slag.

Procedure

Materials Preparation — The VIF was relined before each dip test. To reline the furnace, a layer of refractory fiber paper was placed in the furnace. A one-inch layer of dry ramming refractory was put at the bottom of the furnace. An alumina crucible with a composition of 89% alumina, 10% silica and 1% other oxides was placed in the furnace. Dry ram refractory was packed between the alumina crucible and the refractory paper. The furnace was then topped with refractory plastic. The refractory was dried by heat lamp for 12 hours and then preheated by propane torch before the dip test started. Refractory rods were cored from bricks with a 1.27 cm inner diameter (ID) core drill bit using water as a lubricant. The wet rods were placed in a drying furnace at 105°C. The steel charge chemistry was determined by arc spectroscopy and LECO carbon and oxygen analysis. The steel was then cleaned of oxide by wire brushing. The slag used was created by mixing commercial oxide powders. The slag chemistry was based on commercial slag compositions for ULC steels. FeO was not included in the slag due to its tendency to oxidize carbon from the steel, which counteracted the carbon pickup measurements. The slag was pre-melted in a graphite crucible at 1,350°C. The nominal chemistry of the steel and slag starting materials is shown in Tables 1 and 2, respectively.

Experiment — Refractory dip tests were performed in a VIF to observe the interactions between refractory, steel and slag. The procedure for the dip test was as follows: a 5.5 kg ULC steel charge was placed in the crucible in the VIF. A no-bake sand mold was placed in the pouring area beneath the furnace to collect the steel at the end of the test. A container of Drierite was placed in the chamber to collect any excess moisture. The refractory rod for the dip test was clamped to the end of a maneuverable rod that passed through the top of the VIF chamber. If slag was needed for the test, a pouch made of 1008 steel shim stock containing 110 g slag was placed in the addition cup in Fig. 1a. The O-ring of the chamber door was inspected and cleaned, and the chamber door was closed and sealed. The chamber was evacuated to 67 Pa and then backfilled with ultrahigh-purity (UHP) 99.999% Ar. The chamber was then evacuated to 67 Pa and refilled with UHP Ar a second time. A steady flow of Ar was maintained during the remainder of the experiment and the flow was monitored by a silicone oil bubbler. The VIF was powered up slowly to melt and heat the charge to a target temperature of 1,600°C. If slag was needed for the test, it was added and allowed to melt. The temperature was measured using a type-S immersion thermocouple. A pin sample was taken with an evacuated quartz tube just prior to immersion of the refractory rod. The refractory rod was then dipped approximately 3 cm into the melt. After 1 minute, a pin sample was taken and additional pin samples were then taken every 4 minutes afterward to 30 minutes. The refractory rod was removed from the melt, and a final temperature reading was taken. The steel was

Table 1

Nominal Starting Chemistry of Steel Used in Dip Tests

	C	Si	Al	Ti	Mn	Cu	Cr	Ni	Mo	Fe
Steel (ppm)	34	237	710	492	737	370	365	407	94	Remainder

Table 2

Nominal Starting Chemistries of Slag Used in Dip Tests

	MgO	Al_2O_3	SiO_2	CaO
Unsaturated slag (wt.%)	7.7	34.7	9.9	47.7
MgO-saturated Slag (wt.%)	13.6	32.4	9.3	44.7

then poured into the mold, and the power to the furnace was shut down. The experimental furnace setup is shown in Fig. 1b.

Analysis — The steel pin samples were analyzed using an arc spectrometer. Pieces weighing between 0.6 and 1 g were cut from the pin samples to measure carbon and oxygen by LECO analyses. The refractory samples were sectioned, as shown in Fig. 2, and mounted in epoxy. The refractory surface was polished to 1 µm finish using diamond paste. The polished refractory surface was imaged with a digital camera and by optical microscopy. The polished surfaces were then coated by gold palladium. Scanning electron microscopy (SEM) images and energy-dispersive x-ray spectroscopy (EDX) maps were obtained using an ASPEX SEM.

Results

Carbon pickup from each dip test is shown in Table 3. The SA/V shown in Table 3 is the surface area of refractory in contact with steel divided by the volume of steel. This value fluctuates due to the variation in refractory immersion depth from the dipping method. The aim immersion depth of 3.2 cm was chosen to give an SA/V comparable to an industrial ladle. The initial carbon content of the steel melt also varies somewhat due to variations in the starting material. There was no carbon pickup from 4 wt.% C and 6 wt.% C dip tests that were performed without slag. The 4 wt.% C carbon heats with slag had less pickup than the 10 wt.% C heats with slag. The 4 wt.% C and 10 wt.% C heats with slag had less carbon pickup when the slag contained more MgO. The 10 wt.% C refractory tests were repeated to show reproducibility.

The 10 wt.% C heats show a rapid increase in carbon in the first minute followed by a slower linear increase afterward. This can be seen in Fig. 3. The rapid increase during the first minute was found to be linearly dependent on the surface area of graphite, as shown in Fig. 4. This suggests that the pickup in the first minute is from the dissolution of exposed graphite near the specimen surface during initial steel contact. If this initial stage of carbon pickup is removed from the data, the carbon pickup trend appears to be very similar for all 10 wt.% C refractory dip tests, with the exception of the test with 13.6 wt.% MgO slag. This graph can be seen in Fig. 5.

The 4 wt.% C and 6 wt.% C dip tests without slag both showed no carbon pickup, as shown in Fig. 6. Also shown in Fig. 6, the 12 wt.% C and 10 wt.% C samples have a similar carbon pickup trend. This suggests that there is a fundamental change in the mechanism for carbon pickup between high-carbon bricks and low-carbon bricks.

The 10 wt.% C and the 4 wt.% C refractory dip tests that were performed with a 7.7 wt.% MgO slag both appear to pick up carbon at the same rate. This can be seen clearly in Fig. 7. The 4 wt.% C refractory dip specimen showed much more corrosion at the slagline

Figure 1

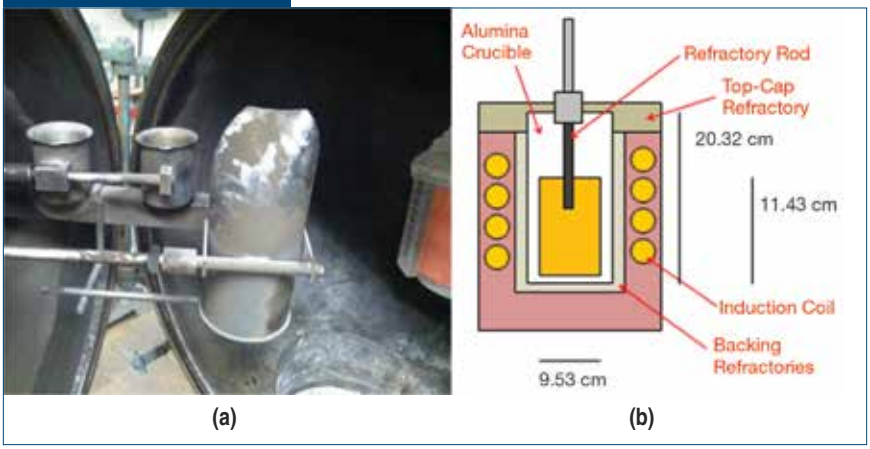

VIF chamber with maneuverable containers used to add slag (a) and experimental setup in the VIF (b).

Figure 2

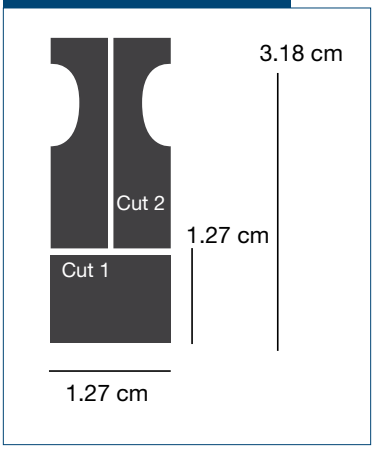

Sectioning refractory dip samples for analysis: Cut 1 was used to observe the refractory in contact with steel. Cut 2 was used to observe the slagline.

Table 3

Carbon Pickup of Experimental Dip Tests

MgO-C refractory wt.% C	Steel wt. (Kg)	SA/V (cm^2/cm^3) *1,000	Slag MgO content (wt.%)	Initial C (ppm)	C pickup (ppm)
4	5.55	21	0	30 ± 5	0 ± 6
4	5.60	28	7.7	44 ± 11	25 ± 13
4	5.45	18	13.6	47 ± 7	23 ± 12
6	5.65	19	0	40 ± 5	0 ± 5
10	5.65	17	0	33 ± 6	60 ± 18
10	5.55	18	0	34 ± 4	45 ± 7
10	5.70	20	7.7	49 ± 3	55 ± 11
10	5.55	16	7.7	50 ± 2	51 ± 8
10	5.60	28	9.6	55 ± 3	69 ± 8
10	5.55	15	13.6	43 ± 9	29 ± 10
12	5.90	14	0	34 ± 5	45 ± 8

Figure 3

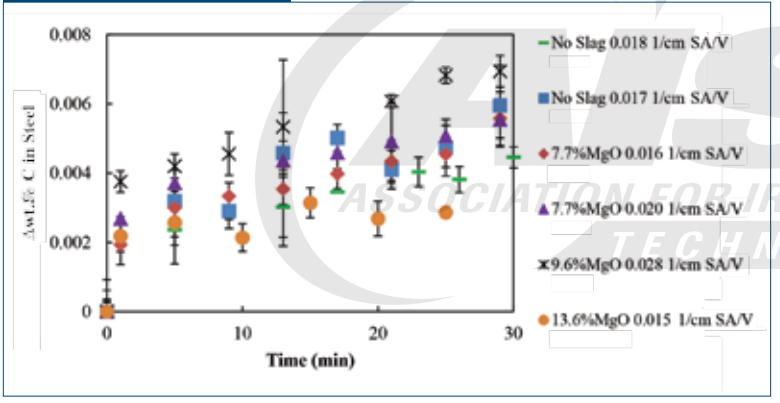

Increase in carbon content of the steel bath vs. time for all 10 wt.% C refractory tests.

Figure 4

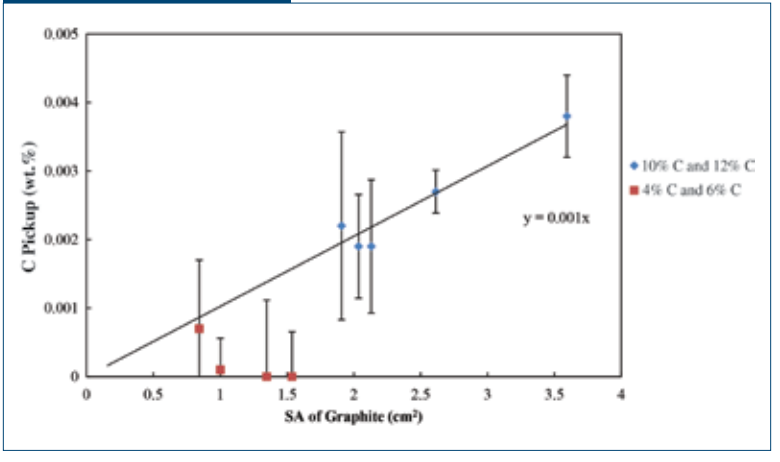

Carbon pickup after the first minute of contact with steel vs. area of exposed graphite.

than the 10 wt.% C dip specimen, which is why the carbon pickup rate is similar despite the lower carbon content of the 4 wt.% C refractory sample. It should be noted that the 4 wt.% C refractory dip test does not show the initial large carbon pickup in the first minute, which was observed in the 10 wt.% C refractory dip test.

Dip tests with 13.6 wt.% MgO slag showed less corrosion of refractory at the slagline. The 4 wt.% C dip test showed an arrest in the carbon pickup at 10 minutes, and the 10 wt.% C dip test showed an arrest in the carbon pickup at 15 minutes. The carbon pickup of these dip tests vs. time is shown in Fig. 8.

Discussion

Carbon pickup from 10 wt.% C and 12 wt.% C refractories can be divided into two stages. The first stage is the rapid increase in carbon seen within the first minute of contact with the steel. The second stage is the slower linear increase of carbon seen in dip tests after the rapid initial pickup. Second stage pickup is seen both with and without slag. The amount of stage one carbon pickup is linearly related to the exposed graphite surface area. This suggests that the source of pickup in the first stage is direct carbon contact at the surface of the refractory that dissolves readily into the steel. An exception to this observed behavior is seen with some 4 wt.% C and 6 wt.% C refractory samples. Fig. 4 indicates that 4 wt.% C and 6 wt.% C refractory samples generally do not have a carbon pickup consistent with their exposed surface area of graphite. The contact between steel and surface carbon on these samples could be limited by the non-wetting nature of liquid steel to MgO, as Khanna et al. and Ohno et al. have observed.[15,18]

The ability for steel to penetrate the pores of a refractory is dependent on the pore size, pressure and interfacial wetting conditions. The critical radius for steel penetration into the refractory is given by:[41]

$$r = \frac{2\gamma \cos\theta}{\rho_{steel} g h} \quad \text{(Eq. 6)}$$

$$P = \rho_{steel} g h \quad \text{(Eq. 7)}$$

where
P = pressure of the liquid steel,
ρ_{steel} = steel density,
h = bath height,
g = acceleration due to gravity,
r = pore radius,
γ = surface tension of liquid steel and
θ = wetting angle between liquid steel and MgO.

For the experiments, the density of liquid steel is 6.98 g/cm^3, the bath height is 3.18 cm, the surface tension for steel (77 ppm oxygen, 90 ppm carbon and 50 ppm sulfur) is 1,632 mN/m[42] and the wetting angle between liquid iron and MgO has been measured to be between 94° and 120°.[43]

The pore radius was measured for the 10 wt.% C refractory to be between 20 and 130 µm, and the pore radius for the 4 wt.% C refractory was measured to be less than 5 µm. The calculated critical pore radius for refractory penetration by steel, using a wetting angle of θ = 94°, is estimated to be about 100 µm for these experiments. Thus, the 10 wt.% C refractory that has a pore size greater than the critical pore size can be penetrated by steel and pick up carbon. In contrast, the 4 wt.% C refractory with a pore size below the critical pore size is not penetrated by steel and therefore cannot pick up carbon. Fig. 9a shows steel penetration observed in a 10 wt.% C refractory sample tested with no slag present. No significant steel penetration was observed on the 4 wt.% C and 6 wt.% C refractory.

The critical pore size calculation suggests that carbon pickup for 10 wt.% C and 12 wt.% C bricks is controlled by penetration and direct dissolution of graphite when no slag is present. This is in agreement with observations in literature.[2,5,7,12–17] No dense MgO layer was observed in the refractory dip test samples. Lehmann et al. reported that the growth of a dense MgO layer in MgO-C refractories is inhibited by Al killing,[5] which is in agreement with the authors' findings. The absence of carbon pickup in the 4 wt.% C and 6 wt.% C refractory dip tests suggests that carbon pickup by a CO

Figure 5

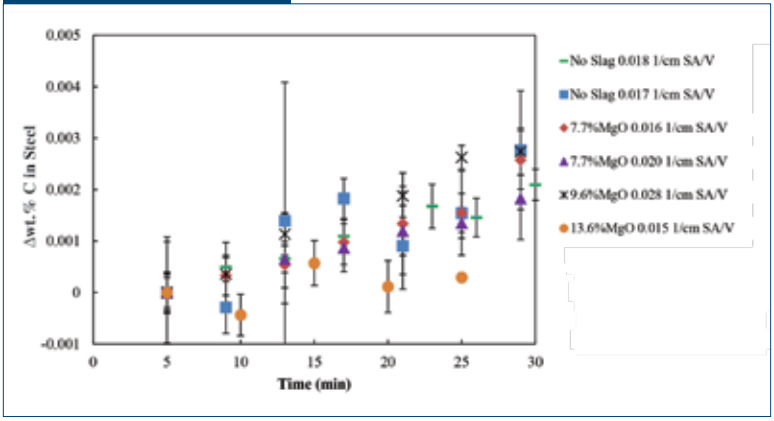

Relative carbon vs. time re-zeroed at five minutes of immersion for all 10 wt.% C refractory tests.

Figure 6

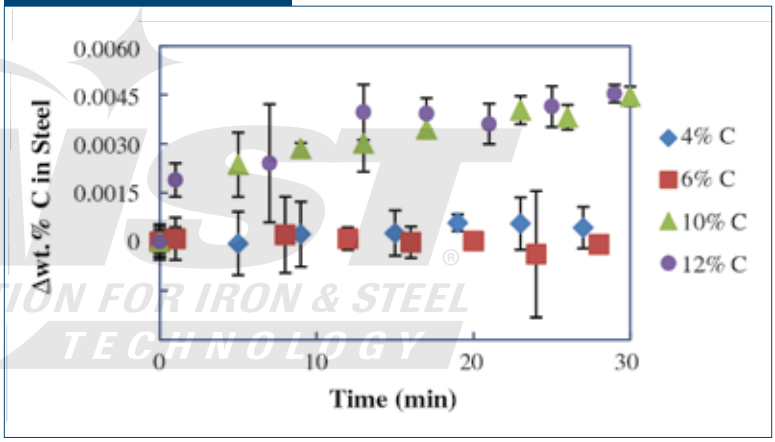

Carbon pickup from MgO-C refractories at four different carbon levels from dip tests performed without slag.

Figure 7

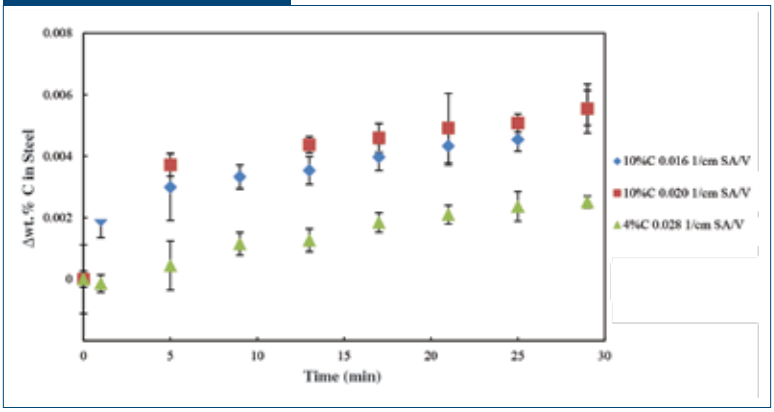

Carbon pickup for 10 wt.% C and 4 wt.% C refractory dip tests with 7.7 wt.% MgO slag.

Figure 8

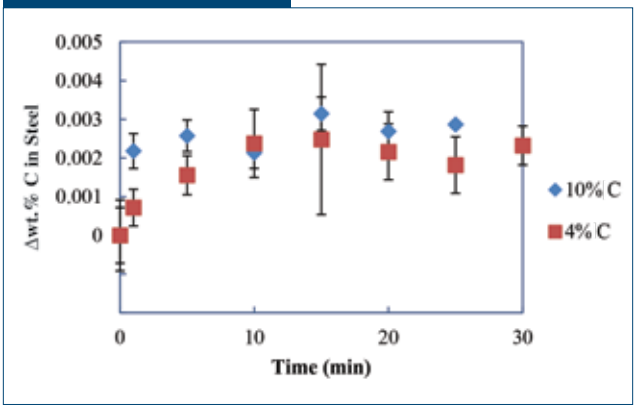

Carbon pickup vs. time for 10 wt.% C and 4 wt.% C dip tests with 13.6 wt.% MgO slag.

Figure 9

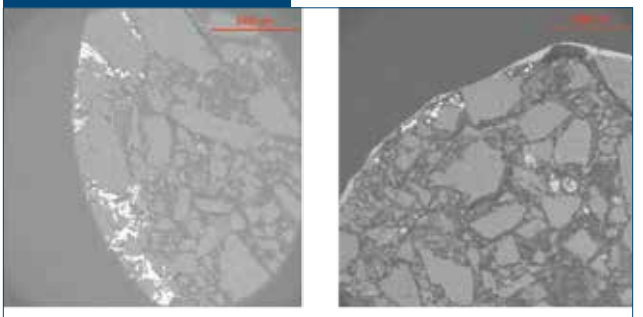

Steel penetration into refractory: 10 wt.% C dip test without slag (a) and 10 wt.% C dip test with MgO-saturated slag (b).

transport mechanism is insignificant in the experiments presented here. This is in contrast with the work of Lehmann et al., who observed that Al-killed steels increase the driving force for CO transport.[5]

The 4 wt.% C and 10 wt.% C dip tests performed with a 7.7 wt.% MgO slag appear to have the same carbon pickup mechanism because they increase in carbon at the same rate. This would indicate a change in mechanism from steel penetration control in the absence of slag to slag corrosion control when slag is present. All samples in contact with slag experienced some amount of notching at the slagline. Slag dissolves MgO at the slagline and steel dissolves the exposed graphite.[10,21,24] It can be seen in Fig. 9b that steel penetration in 10 wt.% C refractory is generally much less when slag is present. It appears that after the surface graphite is dissolved, slag wets the surface of the refractory and inhibits steel penetration. The 10 wt.% C refractories still have some steel penetration, which influences the rate of carbon pickup. It can be seen in Table 4 that the volume corroded decreases significantly when a 10 wt.% C refractory is used rather than a 4 wt.% C refractory. The volume corroded also decreased for the heats with a 13.6 wt.% MgO slag, which lowered the observed carbon pickup after 1 minute. The literature confirms that MgO-saturated slag decreases corrosion.[9,19,23,27] Thus, the corrosion rate of the notch should decrease as slag MgO content approaches saturation. There was still some refractory corrosion in the 13.6 wt.% MgO slag heats because corrosion of the alumina crucible during the experiment changed the solubility of MgO in the slag with time. Tayeb et al. found that increasing alumina increased the solubility of MgO in slag.[30] Table 5 shows the initial slag chemistry for the dip tests, the final chemistry of dip test slags and the MgO

Table 4

Calculated Carbon Pickup of Refractory Dip Tests

MgO-C refractory wt.% C	SA/V *1,000 (cm^2/cm^3)	Slag MgO content (wt.%)	C pickup after 1 minute (ppm)	Volume corroded (cm^3)	C pickup from corrosion (ppm)	C pickup from penetration (ppm)	Calc. C pickup (ppm)
4	28	7.7	26 ± 5	0.869	19	0	19
4	18	13.6	23 ± 12	0.168	4	27*	31
10	17	0	28 ± 15	0	0	24	24
10	18	0	21 ± 13	0	0	23	23
10	20	7.7	29 ± 8	0.309	15	10	25
10	16	7.7	37 ± 12	0.236	12	5	17
10	28	9.6	32 ± 8	0.207	11	27	38
10	15	13.6	7 ± 5	0.032	2	5	7
12	14	0	26 ± 8	0	0	23	23

*slag penetration

Table 5

Final Slag Compositions of Dip Tests

MgO-C refractory wt.% C	State	MgO (wt.%)	Al_2O_3 (wt.%)	SiO_2 (wt.%)	K_2O (wt.%)	CaO (wt.%)	TiO_2 (wt.%)	FeO (wt.%)	MgO saturation (wt.%)
4	Initial	7.70	34.68	9.93	—	47.81	—	—	8.63
	Final	6.08	62.27	4.59	0.10	24.23	2.00	0.64	20.84
4	Initial	13.62	32.41	9.25	—	44.60	—	—	8.64
	Final	11.60	46.88	13.34	0.11	25.21	2.11	0.72	19.43
10	Initial	7.69	34.89	9.96	—	47.75	—	—	8.70
	Final	7.22	55.77	6.19	0.10	28.17	1.94	0.58	18.40
10	Initial	7.70	34.70	9.89	—	47.78	—	—	8.63
	Final	7.13	59.48	4.88	0.11	25.99	1.72	0.62	19.61
10	Initial	9.55	34.00	9.71	—	46.74	—	—	8.65
	Final	9.57	54.69	5.31	0.11	27.23	2.35	0.69	18.62
10	Initial	13.62	32.40	9.25	—	44.63	—	—	8.63
	Final	12.81	51.16	5.23	0.11	27.55	2.42	0.66	17.90

needed to saturate the slags. The MgO saturation level was calculated using Factsage® version 7 and FToxid database. The conditions used for the calculations were 1,600°C and an argon atmosphere with an oxygen partial pressure of 10^{-4}.

Table 4 also shows the calculated carbon pickup based on the amount of penetration and the volume of refractory corrosion. The calculated carbon pickup takes both steel penetration and refractory corrosion into account. The amount of carbon gained through penetration was estimated by calculating the amount of carbon displaced by the penetrated steel in the sample and assuming that all of this carbon entered the steel bath. The amount of carbon from refractory corrosion was estimated by calculating the amount of carbon that was in the corroded volume at the slagline and assuming that all of this carbon entered the steel bath. This volume was calculated by taking the area of the half-ellipse-shaped notch in the refractory and multiplying by the circumference of the rod at the centroid of the notch. The calculated pickup is generally in good agreement with the amount of carbon pickup observed in the experiments when the initial pickup by direct contact during the first minute of exposure is excluded, as shown in Fig. 10.

Figure 10

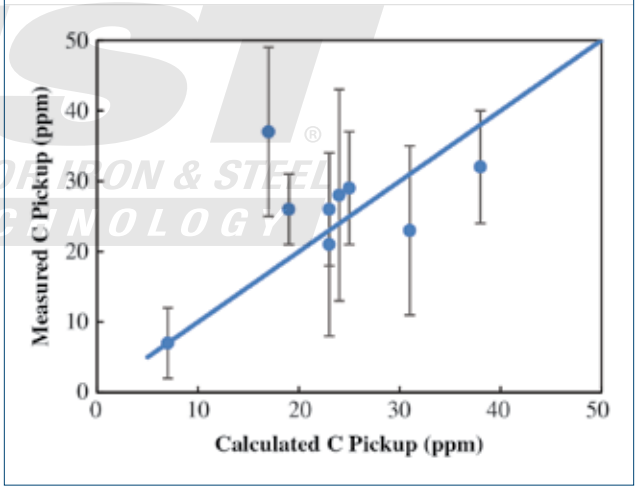

Comparison of calculated and measured carbon pickup from refractory dip tests.

Conclusions

Laboratory dip tests were performed with industrial MgO-C refractory rod samples in ULC steel to investigate mechanisms for carbon pickup. The tests showed the effects of refractory carbon content on the rate of carbon pickup in the presence and absence of slags with varying MgO content. Four different MgO-C refractories were tested: 4 wt.% C, 6 wt.% C, 10 wt.% C, and 12 wt.% C. Three different slag conditions were used: 7.7 wt.% MgO, 13.6 wt.% MgO and no slag. The investigation has shown:

- Carbon pickup in the first minute of contact between steel and refractory for 10 wt.% C and 12 wt.% C refractories is from the dissolution of graphite near the refractory surface by direct contact.
- When no slag is present, carbon pickup after the first minute is controlled by penetration of steel into the refractory and dissolution of graphite by the penetrating steel for 10 wt.% C and 12 wt.% C refractories.

- There is no carbon pickup from 4 wt.% C and 6 wt.% C when there is no slag present because the spacing between MgO grains is too small to allow contact between steel and graphite or penetration of steel into refractory. MgO-C refractories below 6 wt.% C are ideal for the barrel and bottom of ladles because of their resistance to penetration by steel.
- Carbon pickup is controlled by corrosion of refractory by slag at the slagline for dip tests which included slag.
- 4 wt.% C refractories showed greater corrosion than 10 wt.% C. Thus, MgO-C refractories with greater than 10 wt.% C are ideal for the slagline of ladles because of their resistance to slag corrosion.
- 4 wt.% C and 10 wt.% C refractories showed less corrosion when the MgO content of the slag was increased. An MgO saturated slag should be employed to minimize slagline erosion.

Acknowledgments

The authors would like to thank Scott Story and Rakesh Dhaka of United States Steel Corporation, Rod Grozdanich of Spokane Industries, and Bill Headrick of MORCO for their assistance.

References

1. R.E. Showman and K.E. Lowe, "Controlling Carbon Pickup in Steel," *AFS Transactions,* 2010, pp. 385–395.
2. R. Amavis, "3.3 Ultralow Carbon," *Refractories for the Steel Industry,* Springer, 1990, pp. 181–182.
3. C. Jian, Z. Yiyu and Z. Lixin, "Progress of Production Technology of Clean Steel in Baosteel."
4. M.C. Franken, R. Siebring and T.W.M. de Wit, "New Refractory Lining for Steel Ladle BOS' No. 2 Corus IJmuiden," *Unitecr '01,* 2001, pp. 128–138.
5. J. Lehmann, M. Boher, H. Soulard and C. Gatellier, "Metal/Refractory Interactions: A Thermodynamic Approach," *Unitecr '01,* 2001.
6. R. Khanna, M. Ikram-Ul-Haq, Y. Wang, S. Seetharaman and V. Sahajwalla, "Chemical Interactions of Alumina-Carbon Refractories With Molten Steel at 1,823 K: Implications for Refractory Degradation and Steel Quality," *Metallurgical and Materials Transactions,* Vol. 42B, 2011.
7. R. Khanna, J. Spink and V. Sahajwalla, "Role of Ash Impurities in the Depletion of Carbon From Alumina-Graphite Mixtures Into Liquid Iron," *ISIJ International,* Vol. 47, No. 2, 2007, pp. 282–288.
8. T.J. Wilde, M.R. Hatfield and V.J. Nolan, "Carbon as a Refractory," *Transactions of the American Foundrymen's Society,* Vol. 61, 1953, pp. 640–642.
9. S. Akkurt and H.D. Leigh, "Corrosion of MgO-C Ladle Refractories," *American Ceramic Society Bulletin,* Vol. 82, No. 5, 2003, pp. 32–40.
10. Z. Li, K. Mukai and Z. Tao, "Reactions Between MgO-C Refractory, Molten Slag and Metal," *ISIJ International,* Vol. 40, 2000, pp. S101–S105.
11. J. Poirier, "Impact of Refractory Materials on Industrial Process – Steelmaking," *Unitecr '11,* 2011.
12. R. Khanna, F. McCarthy, H. Sun, N. Simento and V. Sahajwalla, "Dissolution of Carbon From Coal-Chars Into Liquid Iron at 1,550°C," *Metallurgical and Materials Transactions,* Vol. 36B, 2005, pp. 719–729.
13. Y. Shigeno, M. Tokuda and M. Ohtani, "The Dissolution Rate of Graphite Into Fe-C Melt Containing Sulfur or Phosphorus," *Transactions of the Japan Institute of Metals,* Vol. 26, No. 1, 1985, pp. 33–43.
14. D. Jang, Y. Kim, M. Shin and J. Lee, "Kinetics of Carbon Dissolution of Coke in Molten Iron," *Metallurgical and Materials Transactions,* Vol. 43B, 2012, pp. 1308–1314.
15. R. Khanna, B. Rodgers, F. McCarthy and V. Sahajwalla, "Dissolution of Carbon From Alumina-Carbon Mixtures Into Liquid Iron: Influence of Carbonaceous Materials," *Metallurgical and Materials Transactions,* Vol. 37B, pp. 623–632.
16. H. Sun, "Analysis of Reaction Rate Between Solid Carbon and Molten Iron by Mathematical Models," *ISIJ International,* Vol. 45, No. 10, 2005, pp. 1482–1588.
17. S. Jansson, V. Brabie and P. Jönsson, "Magnesia-Carbon Refractory Dissolution in Al-Killed Low-Carbon Steel," *Ironmaking & Steelmaking,* Vol. 33, No. 5, 2006, pp. 389–397.
18. K. Ohno, T. Miyake, S. Yano, C.S. Nguyen, T. Maeda and K. Kunitomo, "Effect of Carbon Dissolution Reaction on Wetting Behavior Between Liquid Iron and Carbonaceous Material," *ISIJ International,* Vol. 55, No. 6, 2015, pp. 1252–1258.
19. S. Smets, S. Parada, J. Weytjens, G. Heylen, P.T. Jones, M. Guo, B. Blanpain and P. Wollants, "Behavior of Magnesia-Carbon Refractories in Vacuum-Oxygen Decarburization Ladle Linings," *Ironmaking & Steelmaking,* Vol. 30, No. 4, 2003, pp. 293–300.
20. N. Bannenberg, "Demands on Refractory Material for Clean Steel Production," *Unitecr '95,* 1995.
21. K. Mukai, J.M. Toguri, N.M. Stubina and J. Yoshitomi, "A Mechanism for the Local Corrosion of Immersion Nozzles," *ISIJ International,* Vol. 29, No. 6, 1989, pp. 469–476.
22. L.M. Aksel'rod, O.A. Val'dman, I.Y. Dol'nikov, V.L. Novikov and B.F. Yudin, "Interactions of Steel With Refractories Containing Oxygen Free Additions," *Ogneupory,* No. 10, 1984, pp. 55–58.
23. P. Blumenfeld, S. Peruzzi, M. Puillet and J. de Lorgeril, "Recent Improvements in Arcelor Steel Ladles Through Optimization of Refractory Materials, Steel Shell and Service Conditions," *La Revue de Metallurgie,* 2005.
24. K. Mukai, "Marangoni Flows and Corrosion of Refractory Walls," *Philosophical Transactions: Mathematical, Physical, and Engineering Sciences,* Vol. 356, No. 1739, 1998, pp. 1015–1026.
25. M. Cho, M.V. Ende, T. Eun and I. Jung, "Investigation of Slag-Refractory Interactions for the Ruhrstahl Heraeus (RH) Vacuum Degassing Process in Steelmaking," *Journal of the European Ceramic Society,* Vol. 32, 2012, pp. 1503–1517.
26. J. Potschke and C. Bruggmann, "Premature Wear of Refractories Due to Marangoni-Convection," *Steel Research International,* Vol. 83, No. 7, 2012, pp. 637–644.
27. H. Sunayama and M. Kawahara, "Corrosion Behavior of MgO-C Refractory Accompanied by Bubble Formation in Molten Slag," *9th Biennial Worldwide Congress on Refractories,* pp. 52–56.
28. W.S. Resende, R.M. Stoll, S.M. Justus, R.M. Andrade, E. Longo, J.B. Baldo, E.R. Leite, C.A. Paskocimas, L.E.B. Soledade, J.E. Gomes and J.A. Varela, "Key Features of Alumina/Magnesia/Graphite Refractories for Steel Ladle Lining," *Journal of the European Ceramic Society,* Vol. 20, 2000, pp. 1419–1427.
29. S. Parada, M. Guo, P.T. Jones, B. Blanpain and P. Wollants, "Chemical Wear Mechanism of Magnesia-Chromite and Magnesia-Carbon Refractories Exposed to Stainless Steelmaking Slags," *9th Biennial Worldwide Congress on Refractories,* pp. 63–67.
30. M.A. Tayeb, A.N. Assis, S. Sridhar and R.J. Fruehan, "MgO Solubility in Steelmaking Slags," *Metallurgical and Materials Transactions,* Vol. 46B, 2015, pp. 1112–1114.

31. M. Guo, S. Parada, P.T. Jones, J. Van Dyck, E. Boydens, D. Durinck, B. Blanpain and P. Wollants, "Degradation Mechanisms of Magnesia-Carbon Refractories by High-Alumina Stainless Steel Slags Under Vacuum," *Ceramics International,* Vol. 33, 2007, pp. 1007–1018.
32. M. Guo, S. Parada, P.T. Jones, E. Boydens, J.V. Dyck, B. Blanpain and P. Wollants, "Interaction of Al_2O_3-Rich Slag With MgO–C Refractories During VOD Refining — MgO and Spinel Layer Formation at the Slag/Refractory Interface," *Journal of the European Ceramic Society,* Vol. 29, 2009, pp. 1053–1060.
33. L. Musante, P.G. Galliano, E. Brandaleze, V. Muñoz and A.G.T. Martinez, "Chemical Wear of Al_2O_3-MgO-C Bricks by Air and Basic Slags," *Unitecr '13,* 2013, pp. 596–602.
34. X. Li, B. Zhu and T. Wang, "Effect of Electromagnetic Field on Slag Corrosion Resistance of Low-Carbon MgO-C Refractories," *Ceramics International,* Vol. 38, 2012, pp. 2105–2109.
35. J. Potschke and T. Deinet, "Premature Corrosion of Refractories by Steel and Slag," *Millenium Steel,* 2005, pp. 109–113.
36. I. Bae, J. No, C. Um and M. Shin, "The Improvement of Casting Ladle Lining for Clean Stainless Steel Production," *Unitecr '07,* 2007.
37. M. Ikram-Ul-Haq, R. Khanna, P. Koshy and V. Sahajwalla, "High-Temperature Interactions of Alumina-Carbon Refractories With Molten Iron," *ISIJ International,* Vol. 50, No. 6, 2010, pp. 804–812.
38. M.Y. Solar and R.I.L. Guthrie, "Kinetics of the Carbon-Oxygen Reaction in Molten Iron," *Metallurgical Transactions,* Vol. 3, 1972, pp. 713–722.
39. P. Tassot, D. Verrelle and M. Puillet, "Optimization of Refractories of Steel Ladles With Regard to Process Conditions at SOLLAC Dunkirk and Florange."
40. A. Sen, J.K. Sahu and J.N. Tiwari, "Studies and Optimization of Various Types of Zirconia to Minimize Crack Propagation and Improve Corrosion and Erosion Resistance of Slag Band of Subentry Nozzle," *Unitecr '13,* 2013, pp. 752–757.
41. D.M. Stefanescu, M.D. Owens, A.M. Lane, T.S. Piwonka, K.D. Hayes and J.O. Barlow, "Penetration of Liquid Steel in Sand Molds Part 1: Physics and Chemistry of Penetration and Mathematical Modeling – Metal Side," *AFS Transactions,* 2001.
42. F.A. Halden and W.D. Kinger, "Surface Tension at Elevated Temperatures II Effect of C, N, O, and S on Liquid Iron Surface Tension and Interfacial Effect of C, N, O, and S on Liquid Iron Surface Tension Energy With Al_2O_3," 1955.
43. C. Xuan, H. Shibata, S. Sukenaga, P.G. Jansson, K. Nakajima, "Wettability of Al_2O_3, MgO and Ti_2O_3 by Liquid Iron and Steel," *ISIJ International,* Vol. 55, No. 9, 2015, pp. 1882–1890. ✦

To nominate this paper for the AIST Hunt-Kelly Outstanding Paper Award, visit AIST.org/huntkelly.

This paper was presented at AISTech 2016 — The Iron & Steel Technology Conference and Exposition, Pittsburgh, Pa., USA, and published in the Conference Proceedings.